# MODEL PATHWAYS FOR GAS RELEASE FROM LIGNITES

by
M.T. Klein and P.S. Virk
Department of Chemical Engineering
Massachusetts Institute of Technology
Cambridge, MA 02139

## Introduction:

Recent developments limiting petroleum supplies have intensified the search for other sources of energy and chemical feedstocks. Two such alternatives are coal, of which lignites are especially abundant in the U.S. (1), and those renewable resources termed biomass, of which lignin is a major component (2). Commercial methods for processing both coal and biomass invariably involve high temperature treatments, aspects of which have been investigated in many laboratory pyrolyses of lignin and lignites (3-5). Unfortunately, the basic pathways and reaction mechanisms involved in these pyrolyses have remained obscure, on account both of the refractory nature of the substrates and the lack of unequivocal chemical structures to describe them. Pyrolyses of several very simple lignin-related substrates have also been reported, notably by Russian investigators (6-11). Among these, the pyrolyses of anisole and guaiacol (6-9) have been interpreted (11) in terms of analogous free radical demethylation and demethoxylation mechanisms which describe the formation of the observed gaseous products, methane and carbon monoxide, but are unable to rationalize the corresponding observed liquid products, benzene, phenol, and catechol. Overall, the literature still provides no framework, either theoretical or experimental, for modelling gas release during pyrolysis of lignites and lignin. This motivated the present work.

Our investigation derives from two hypotheses. First, the primary evolution of gas during lignite pyrolysis is presumed to occur from lignin-related residues in the coal. Second, it is hypothesized that the molecular topology of lignoid structures favors elimination of gases by concerted pericyclic reactions which are thermally (i.e., ground state)-allowed. In regard to the first hypothesis, the evolutionary link between biomass and coal is relatively well established (12,13) with lignin akin to peat, which is adjacent to lignite in the coalification series. It is therefore quite reasonable to expect lignin-related residues in lignite; indeed, such residues can be recognized in most structural models (1 ,14) of this coal. Our second hypothesis, which has not hitherto been mooted, is based on analysis of the Freudenberg model of lignin (2) in light of the Woodward-Hoffman (15) description of thermal pericyclic reactions. Such analyses revealed a variety of lignoid chemical moieties susceptible to pyrolysis by pericyclic pathways that involve elimination of gaseous products such as methane, carbon monoxide, carbon dioxide and water. According to the pericyclic formalism, methane might originate by concerted 6e($\sigma\pi\sigma$) group-transfer elimination from a guaiacyl moiety:

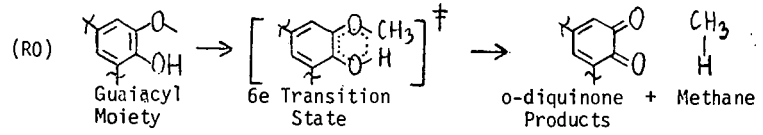


The guaiacyl moiety is relatively abundant in the lignin structure itself, within coniferyl alcohol monomer units which have suffered polymerization in the 5 and/or β positions; guaiacyl moieties can also arise from reversion of the prevalent β-ether linkage between monomer units. In similar vein, carbon monoxide could arise by cheletropic extrusion of a carbonyl unit, such as that in coniferaldehyde,

and carbon dioxide by cyclo-reversion of lactones and aryl-carboxylic ("humic") acids. Finally, pericyclic elimination of water could result from retro-ene reactions among the guaiacyl-glycerol units in lignin, possibly following β-ether reversion.

The preceding hypotheses for gas release from lignites are amenable to experimental probing by pyrolysis of appropriate model compounds. In the present paper we report preliminary results for two series of substrates respectively associated with methane and with carbon monoxide production. Methane formation was examined by pyrolyses of guaiacol, the prototypical guaiacyl moiety, along with anisole (control), and a number of substituted guaiacols, including 2,6 dimethoxyphenol, isoeugenol, and vanillin. Carbon monoxide release was investigated by pyrolysing benzaldehyde, the prototypical moiety, along with related carbonyl compounds including acetophenone (control), cinnamaldehyde and vanillin, the latter two respectively intended to illustrate the effects of extended conjugation and guaiacyl substitution.

Experimental:

The substrates pyrolysed were all commercially available in purities exceeding 98% and were used as received. The batch reactors employed were stainless steel "tubing bombs", fashioned from Swagelok components and ranging in volume from 0.6 to 10.5 $cm^3$. The larger reactors were equipped with valves for gas sampling, while the smaller reactors were used to minimize heat-up and quench times in experiments of short duration. Kinetic data were demonstrably unaffected by variations in reactor volume. All reactors were loaded and sealed in a glove box maintained with an inert atmosphere of either nitrogen or argon, the inert serving as an internal standard in later gas analyses. The reactors were then immersed in a fluidized sand bath for the duration of reaction and finally quenched in an ice water bath. The pyrolysis experiments were conducted at temperatures from 250 to 600 C, with holding times of 2 to 40 minutes. Substrate conversions were generally held to less than 30%, in an effort to emphasize primary reactions; however, kinetic data were also obtained at very low conversions, of < 10% for some substrates which were prone to form coke, and at high conversions, up to 90%, in other selected instances. The amount of substrate charged varied from 10 to 200 mg, to provide initial substrate concentrations ranging from 0.15to 3.0 mol/ℓ in the gas phase. Product analyses were effected by gas chromatography on a Hewlett-Packard 5730 instrument. Gaseous products, sampled by syringe, were analysed on molecular sieve, silica gel, and Porapak Q columns using helium carrier gas and thermal conductivity detectors. Liquid and solid reactor contents were dissolved in solvent and analysed on Porapak P and Q, and silicone oil columns, using either thermal conductivity or flame-ionization detection. Care was taken to effect material balance closures and to match gas and liquid product yields. In all cases, the liquid (and solid) phase material balance, which invariably included unreacted substrate, could be closed to within ±10%. In favorable cases, where reaction stoichiometry was known, the absolute gas and liquid products agreed to within ±10% of each other and separately equalled the amount of substrate converted. However in certain other cases, noted in the text, reaction stoichiometry was uncertain and precise matching of gaseous and liquid products impossible; in such instances, substrate decomposition kinetics were based on liquid phase analyses.

Results:

Table 1 summarizes the present experimental grid. For each substrate pyrolysed, the table lists chemical structure, purity, and reaction conditions of temperature, holding time and concentration. The experimental results will be described in three parts, namely (i) prototype pyrolyses, of guaiacol and benzal-

dehyde, which revealed major pathways for methane and carbon monoxide formation, (ii) substituenteffects, inferred from pyrolyses of substituted guaiacols and benzaldehydes, and (iii) control pyrolyses, of the relatively refractory substrates anisole and acetophenone, for comparisons with the prototype pyrolyses.

(i) Prototype Pyrolyses

Guaiacol pyrolysis yielded methane, carbon monoxide,catechol and phenol as the only products at low conversions; at high conversions a solid 'coke' also formed, being accompanied by reduced yields of catechol relative to the other products. Relationships among products are illustrated in Figure 1. The mol ratios of (methane/catechol), Figure 1a, and (carbon monoxide/phenol), Figure 1b, were each separately close to unity in essentially all cases, covering fractional substrate conversions $0.5 \times 10^{-3} < X < 0.10$ at all temperatures from 250 to 450 C. Also, the mol ratios of ($CO/CH_4$) and (phenol/catechol) were each substantially independent of substrate conversion at any given temperature, as shown in Figure 1c. These observations suggest two parallel pathways for guaiacol decomposition, respectively termed (R1) and (R2):

(R1) 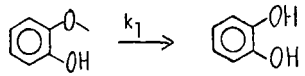 + $CH_4$ (-2H)

(R2) 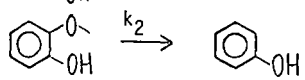 + CO (+2H)

The parentheses to the right of each expression indicate the difference in hydrogen atoms between the substrate and the observed pair of stable products. The order of reactions (R1) and (R2) with respect to guaiacol was examined by varying the initial substrate concentration from 0.45 to 3.0 mol/l in a series of experiments at T = 350C. These data are displayed in Figure 2, parts a, b, and c of which respectively plot the variation with time of guaiacol, catechol, and phenol concentrations, each normalized by the initial guaiacol concentration. On the co-ordinates of Figure 2, a reaction with rate expression $r = kC^{\alpha}$ , i.e. rate constant k and order $\alpha$ ,would yield an initial slope $|\, d\ln (C/C_0)/\, dt|_{\, t \to 0} = kCo^{\alpha-1}$ . In each of Figures 2a, 2b, and 2c, a single average slopesufficed to describe all of the data. No systematic variation of initial slope with initial substrate concentration could be discerned and the absolute uncertainties in the slope, respectively $\pm$20% in Figures 2a and 2b and $\pm$50% in Figure 2c, were small relative to the seven-fold range of initial concentrations used. The foregoing show that $\alpha$=1 for each of reactions (R1) and (R2); that is, the kinetics of guaiacol disappearance, catechol appearance, and phenol appearance were all essentially first order in guaiacol. Further study of guaiacol pyrolyses at temperatures from 300 to 525 C with fixed initial concentration 0.45 mol/l revealed the temperature-dependence of the first order rate constants $k_1$ and $k_2$ respectively associated with reactions (R1) and (R2). These results are shown in Figure 3, an Arrhenius diagram with co-ordinates of $\log_{10}k$ ($s^{-1}$) vs. reciprocal temperature $\theta^{-1}$ where $\theta = 4.573 \times 10^{-3}$ T in Kelvins; on these co-ordinates, the usual Arrhenius relationship describes a straight line, $\log_{10}k = \log_{10}A - E^*/\theta$, where the pre-exponential factor A has units of the rate constant k and the activation energy $E^*$ is expressed in kcal/mol. In Figure 3 it is evident that $\log_{10}k_1$ (shown by circles) increases linearly with decreasing reciprocal temperature $\theta^{-1}$, obeying an Arrhenius relationship over a range of five orders of magnitude in $k_1$. The best fit of these data yields Arrhenius parameters of ($\log_{10}A$ ($s^{-1}$), $E^*$ (kcal/mol)) = (10.9 $\pm$ 0.5 , 43.7 $\pm$ 1.4) for the reaction (R1). Also in Figure 3, $\log_{10}k_2$ (squares) is seen to increase linearly with $\theta^{-1}$ over a range

of four orders of magnitude in $k_2$ and this provides the Arrhenius parameters ($\log_{10}$A ($s^{-1}$), E* (kcal/mol)) = (11.5 ± 0.5, 47.4 ± 1.6) for reaction (R2). These results also reveal that the selectivity of ($CO/CH_4$) formation from guaiacol, given directly by the ratio ($k_2/k_1$), was typically on the order of $10^{-1}$ but increased with increasing temperature, from 0.05 at 300C to 0.25 at 450C.

Benzaldehyde pyrolysis yielded carbon monoxide and benzene as the major products; traces of biphenyl and phenolic products were also detected, their concentration being from one to two orders of magnitude less than that of benzene. The mole ratio of (CO/benzene) products was unity, 1.0 ± 0.1, while the mols of CO and of benzene formed each closely equalled the moles of benzaldehyde that disappeared in all cases, covering fractional substrate conversions from 0.01 to 0.30 at temperatures from 300 to 550C. Thus the benzaldehyde pyrolysis pathway was evidently:

(R3) 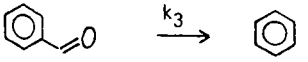 + CO

Variation of the initial substrate concentration from 0.45 to 3.0 mol/ℓ at T = 400C showed reaction (R3) to be strictly first order in benzaldehyde, with the rate constant $k_3 = (8.0 \pm 2.0) \times 10^{-3}\ s^{-1}$ essentially independent of concentration. Finally, measurements of reaction (R3) kinetics at temperatures from 300 to 500C provided the data shown in Figure 4, an Arrhenius plot. It is evident that $\log_{10} k_3$ (circles) increased linearly with decreasing $\theta^{-1}$, the best fit Arrhenius parameters being ($\log_{10}$ A ($s^{-1}$), E* (kcal/mol)) = (9.5 ± 0.8, 41.5 ± 2.7).

(ii) Substituent Effects

Pyrolyses of 2,6 dimethoxyphenol, iso-eugenol, vanillin, and t-cinnamaldehyde probed the effect of substituents on the prototype pathways described above.

Both of the 2,6 dimethoxyphenol and iso-eugenol substrates decomposed clearly by pathways (R1) and (R2) analogous to guaiacol to yield methane, carbon monoxide, and the corresponding liquid products, namely:

(R1) 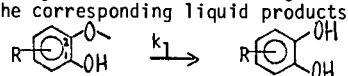 + $CH_4$ (-2H)

(R2) 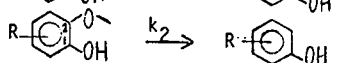 + CO (-2H)

where the substituent R is either 6-methoxy or 4-propenyl. The associated kinetic results are summarized in Table 2 which gives a matrix of first order rate constants, $\log_{10}k$ ($s^{-1}$), obtained at 400C for each substrate decomposing by each prototype pathway. In Table 2, values of $k_1$ and $k_2$ obtained for each of 2,6 dimethoxyphenol and iso-eugenol are close to the corresponding values for guaiacol. That is, the kinetics of both methane and carbon monoxide formation from these two substituted guaiacols were very similar to those from guaiacol itself.

Vanillin pyrolysis yielded CO and methane as the principal gaseous products, the former predominant. Among liquids, at low conversions, guaiacol and dihydroxybenzaldehyde were major products, the former predominant, while at higher conversions catechol also arose, along with lesser amounts of phenol; at the highest conversions solid coke formed. At conversions of $0.02 < X < 0.20$, the mol ratios of (CO/guaiacol) and ($CH_4$/dihydroxybenzaldehyde) were each approximately unity; the latter pair of products were always less than the former at low conversions, with the ratio $(CH_4/CO)_{X\to 0} \sim 0.1$ at T = 400C. These data suggest that vanillin decomposed by pathways of the type (R3) and (R1) earlier established for benzaldehyde and guaiacol:

(R3) 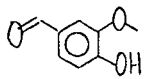 $\xrightarrow{k_3}$  + CO

(R1) 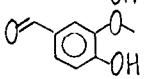 $\xrightarrow{k_1}$ 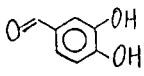 + $CH_4$ (-2H)

At high substrate conversions, the guaiacol and dihydroxybenzaldehyde products could further decompose by the same kinds of pathways to yield the catechol and phenol products observed. Kinetic data for vanillin pyrolysis at 400°C are summarized in Table 2. It is noteworthy that the rate constant $k_3$ for vanillin far exceeded that for benzaldehyde while the rate constant $k_1$ was essentially equal to that from guaiacol. Thus the rate of arylaldehyde decarbonylation was markedly enhanced by the guaiacyl substituents while the rate of guaiacyl demethanation was virtually unaffected by the carbonyl substituent.

Pyrolysis of t-cinnamaldehyde yielded CO as the major gaseous product, with much smaller amounts of hydrogen, methane, and acetylene also detected. A number of liquid products arose among which a dimeric condensation product, phenols, plus cresols, and styrene, were each appreciable, along with lesser amounts of toluene, benzene, other alkyl benzenes and biphenyl. Product pathways for this pyrolysis have not yet been fully established. However it was significant that the mol ratio of (CO/styrene) products always approached unity at low substrate conversions and the kinetics of styrene appearance were essentially first order in substrate over a three-fold range of initial concentrations at 350°C. This allows tentative isolation of a pathway of type (R3) for CO formation from cinnamaldehyde:

(R3) 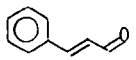 $\xrightarrow{k_3}$  + CO

The first order rate constant $k_3$ for cinnamaldehyde, shown in Table 2, was about three-fold greater than that for benzaldehyde, suggesting that decarbonylation rates are enhanced by conjugation.

(iii) Control Pyrolyses

Anisole pyrolysis produced methane and carbon monoxide as the major gaseous products with hydrogen also present in appreciable amounts. The major liquid products were ortho-cresol, phenol, and benzene, with smaller amounts of toluene, xylenes, and xylenols also detected. At low substrate conversions, the product proportions were strongly influenced by reaction temperature. Thus at 400°C it was found that $CH_4$:CO::1.0:0.4 and o-cresol:phenol:benzene::3:1:0.1, whereas at 550°C these ratios were $CH_4$:CO::1:1 and o-cresol:phenol:benzene::0.6:1:1. Among products, the ratios $_4$ (methane/phenol) = 0.2 ± 0.1 and (CO/benzene) = 0.6 ± 0.2 were roughly constant at substrate conversions $0.01 < x < 0.30$ and T = 450°C. Anisole pyrolysis thus appears to involve at least three major pathways, namely, re-arrangement to o-cresol, formation of methane and phenol, and the formation of CO and benzene. Further experiments at T = 450°C and spanning initial substrate concentrations from 0.45 to 3.1 mol/ℓ showed that the overall substrate disappearance, as well as the normalized phenol and benzene product appearances, were all essentially first order in anisole. This allowed association of a first order rate constant with the overall anisole disappearance, termed reaction (R4):

(R4)  $\xrightarrow{k_4}$ all products

where (R4) is, of course, a sum of the individual anisole decomposition pathways identified above but not as yet decisively delineated. Study of (R4) at various temperatures provided the values of $k_4$ depicted in figure 3 (diamonds ); the corresponding Arrhenius parameters for overall anisole decomposition are

$(\log_{10}A(s^{-1}),\ E^*(kcal/mol)) = (12.1\pm 0.8,\ 51.4 \pm 2.4)$. The value of $k_4$ for anisole at T = 400°C is also quoted in Table 2, for comparison with guaiacol. From Figure 3 and Table 2 it is clear that the overall anisole decomposition by (R4) was typically at least an order of magnitude slower than guaiacol decomposition by (R1) in the present experiments. Exact comparisons between the kinetics of $CH_4$ and CO formation from guaiacol and from anisole cannot yet be made but the data suggest that both gases form roughly a hundred times faster from the former substrate.

Acetophenone pyrolysis led to carbon monoxide and methane as the major gaseous products with $(CO/CH_4) \sim 2$; hydrogen was also present. Liquid product spectra were complex, benzene, toluene, xylenes and styrene being the major components, along with apparent dimers; additionally present were benzaldehyde, biphenyl, cresols, and aromatic ethers. No clear link has yet been established between gas and liquid products, precluding enunciation of possible pyrolysis pathways. The overall decomposition of acetophenone was found to be roughly first order in substrate at T = 550°C for initial concentrations from 0.14 to 1.4 mol/ℓ. This allows use of a first order overall decomposition pathway of type (R4):

(R4) 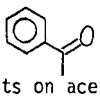 $\xrightarrow{k_4}$ all products

Experiments on acetophenone pyrolyses at various temperatures yielded the values of the rate constant $k_4$ shown in Figure 4 (diamonds ); the corresponding Arrhenius parameters for overall acetophenone decomposition are

$(\log_{10}A(s^{-1}),\ E^*(kcal/mol)) = (10.3 \pm 1.6,\ 50.7 \pm 5.8)$. A value of $k_4$ for acetophenone at 400°C is given in Table 2, for comparison with benzaldehyde. From Figure 4 and Table 2 it can be seen that overall acetophenone decomposition by (R4) is more than two orders of magnitude slower than benzaldehyde decomposition by (R3) in the present experiments.

Discussion:

Comparisons of the present results with previous literature is possible only in a few instances. Prior studies of guaiacol pyrolysis (8-10) provide no activation parameters but do give overall decomposition rate constants $\log_{10}k(s^{-1}) = -1.0$ at 500C and ~0 at 540C which are of the order of magnitude of our $\log_{10}k_1$ for guaiacol in that temperature range. An earlier study of benzaldehyde pyrolysis (16) yielded an overall decomposition rate constant $\log_{10}k(s^{-1}) = -2.2$ at 550C which agrees with our value of $\log_{10}k_3 = -2.3$ at 550C. Two prior anisole pyrolysis (6,7) at 500C yield overall decomposition rate constants $\log_{10}k(s^{-1}) = -1.8$ and $-1.9$ which compare favorably with our value of $\log_{10}k_4 = -2.5$ at 490C. Also, an anisole pyrolysis (17) at 800C showed a product spectrum akin to ours but with the ratio of $(CO/CH_4)$ and (benzene/phenol) each ~3, which accords with our observations showing these ratios to increase from ~0.3 at 350C to ~1.0 at 550C. In summary, pyrolysis data from the present study are in reasonable agreement with the available literature for guaiacol, benzaldehyde and anisole, lending credence to our experimental methods and hence to those results reported here for the first time.

The kinetic data obtained invite mechanistic interpretations. First, in regard to methane formation, guaiacol and anisole offer striking contrasts. The former substrate produced methane at rates a hundred times faster than the latter; also, methane formation from guaiacol was stochiometrically linked with production of catechol whereas that from anisole was associated with appreciably less than stochiometric amounts of phenol; finally, the products from anisole pyrolysis included numerous methyl-benzenes and methyl-phenols, suggestive of radical methylation, whereas such products were absent from guaiacol pyrolyses. Thus the guaiacol evidently had access to a methane-forming pathway that was far more facile than the radical pathway likely responsible (11) for methane formation from anisole. A possible pericyclic reaction path accessible to guaiacol, but not to anisole, involves the concerted group transfer shown in (R0). Here the experimental activation parameters obtained for (R1), which was first order with ($\log_{10}$A, E*) = (10.9, 43.7), are relevant. The value of $\log_{10}$A implies a tight transition state with activation entropy $\Delta S^{\ddagger}$ = -12 cal/mol K; this is close to the magnitude expected for the loss of two bond rotations that must accompany guaiacyl moiety alignment for concerted methane elimination. Further, the observed activation energy for (R1) is close to the values of 45±3 kcal/mol that have been reported for isoelectronic group transfer eliminations of hydrogen and methane from various 1,4 cyclohexadienes (18). Finally, if (R1) is indeed pericyclic like (R0), then its kinetics should be dominated by frontier orbital interactions between the methane and o-diquinone products. However, methane has a relatively large HOMO-LUMO energy gap, while the diquinone, which is further conjugated, must have a small HOMO-LUMO separation. Thus the dominant frontier orbital energy differences, of the form HOMO(methane)-LUMO(diquinone) and v.v., should be relatively large and only little influenced by substituents on the diquinone. Experimentally, it was seen in Table 2 that the kinetics of methane formation from guaiacol were insensitive to substituents. Turning next to carbon monoxide formation, it was clear that benzaldehyde produced CO via (R3) far faster than acetophenone, which latter yielded a product spectrum suggestive of a radical decomposition. In regard to benzaldehyde, we suspect that the pathway (R3) might involve a non-linear cheletropic mechanism (15), with the concerted shift of hydrogen, as in the aldehyde, being more facile than that of methyl, as in the ketone. Although molecular mechanisms for CO release from benzaldehyde have previously been mentioned (16,17), cheletropic extrusions specifically have not hitherto been proposed. In the present case, Arrhenius parameters for the first order forward reaction (R3), namely ($\log_{10}$A, E*) = (9.5, 41.5), can be combined with thermochemical data of ($\Delta H_r$(kcal/mol), $\Delta S_r$(cal/mol K)) = (2.3, 25.5) to provide activation parameters for the bimolecular reverse reaction, namely ($\log_{10}$A (ℓ/mol s), E*) = (5.7, 39.2). The reverse of cheletropic extrusion is, of course, cheletropic addition, which is well known (15,19) to possess tight transition states akin to cycloaddition. It is therefore interesting that the parameters inferred for the reverse of reaction (R3) yield an activation entropy $\Delta S^{\ddagger}$ = -36 cal/mol K, of magnitude typically encountered in cycloadditions. Also, cheletropic decarbonylation reactions are reported in the literature (20) to exhibit great sensitivity to stereoelectronic factors and indeed the present kinetic data showed CO formation to be appreciably affected by modifications of the benzaldehyde structure to vanillin and cinnamaldehyde. The foregoing arguments suggest that pericyclic group transfer elimination and cheletropic extrusion constitute plausible reaction mechanisms for methane and carbon monoxide formation respectively from guaiacol and benzaldehyde pyrolyses.

Acknowledgement:

This work was financially supported by the US DOE through seed funds distributed by the MIT Energy Laboratory.

References:


1. Wender, I., ACS Div. Fuel Chem. preprints, 20(4) 16(1975)

2. Freudenberg, K. and Neish, A.C., Constitution and Biosynthesis of Lignin, Springer-Verlag, New York (1968)

3. Allan, G.G. and Mattila, T., in Sarkanen, K.V. and Ludwig, C.H., ed., Lignins Occurrence, Formation, Structure and Reactions, Wiley Interscience, New York (1971)

4. Suuberg, E.M., Sc.D. Thesis, M.I.T., August 1977

5. Solomon, P.R., ACS Div. Fuel Chem. preprints, 24(3), 154-9(1979)

6. Obolentsev, R.D., J. Gen. Chem. (U.S.S.R.) 16, 1959-70(1946)

7. Friedlin, L.Kh; Balandin, A.A; Nazarova, N.M; Izvest. Akad. Nauk S.S.S.R., Otdel Khim. Nauk ,no. 1, 102-9(1949)

8. Shaposhnikov, Yu. K. and Kosyukova, L.V., Khim. Pererabotka Drev., Ref. Inform., no. 3, 6-9 (1965)

9. Kravchenko, M.I.; Kiprianov, A.I.; Korotov, S. Ya; Nauch. Tr. Leningrad Lesotekh. Akad., 135(2), 60-4(1970)

10. Kiprianov, A.I. and Kravchenko, M.I., Izv. Vyssh. Ucheb. Zaved., Les Zh. 15(5), p121-5(1972)

11. Kislitsyn, A.N.; Rodionova, Z.M.; Savinykh, V.I.; Ill'ina, E.I.; Abakhumov, G.A., Sb. Tr., T sent. Nauch - Issled. Prockt. Inst. Lesokhim. Prom., no. 22, p4-16 (1971)

12. Flaig, W., Chemistry of Humic Substances in Relation to Coalification, in Coal Science, Advances in Chemistry Series, ACS, Wash., D.C. (1966)

13. van Krevelen, D.W., Coal, Elsevier, Amsterdam (1961)

14. Hill, G. and Lyon, L., Ind. Eng. Chem., 54(6), 30-9(1962)

15. Woodward, K.B. and Hoffmann, R., The Conservation of Orbital Symmetry, Verlag Chimie, Academic Press, Germany (1971)

16. Smith, R.E. and Hinshlewood, C.N., Proc. Roy. Soc., (London)A, 175, 131-142 (1940)

17. Ingold, K.V. and Lossing, F.P., Can. J. of Chem., 31, 30-41(1953)

18. Frey, H.M., and Walsh, R., Chem. Rev., 69 103(1969)

19. Mock, W.L. in Pericyclic Reactions Volume II, A.P. Marchand and R.E. Lehr, Editors, Academic Press, New York (1977)

20. Clarke,S.C. and Johnson,B.L., Tetrahedron, 27,3555-61(1971)

Table 1. Experimental Grid

| Set | Substrate | Structure | Purity wt% | Reaction Conditions: Temperature Range C | Holding Times s | Initial Concentration mol/l |
|---|---|---|---|---|---|---|
| 1 | Guaiacol | | 99 | 250-525 | 110-6000 | 0.46-3.07 |
| 2 | Benzaldehyde | | 99 | 300-500 | 120-3600 | 0.16-3.3 |
| 3 | 2,6 dimethoxyphenol | | 99 | 300-500 | 120-1800 | 0.32 |
| 4 | Iso-eugenol | | 99 | 300-500 | 60-1560 | 0.33 |
| 5 | Vanillin | | 99 | 300-500 | 120-1500 | 0.85 |
| 6 | t-Cinnamaldehyde | | 99 | 250-400 | 120-1500 | 0.38-1.3 |
| 7 | Anisole | | 98 | 344-550 | 180-1500 | 0.46-3.07 |
| 8 | Acetophenone | | 98 | 350-550 | 120-4980 | 0.14-1.4 |

Table 2. Summary of Kinetic Data at 400C

| Set | Substrate | Pathway: / Rate Constant: | R1 $\log_{10}k_1$ | R2 $\log_{10}k_2$ | R3 $\log_{10}k_3$ | R4 $\log_{10}k_4$ |
|---|---|---|---|---|---|---|
| 1 | Guaiacol | | -3.2 | -3.8 | - | - |
| 2 | Benzaldehyde | | - | - | -3.7 | - |
| 3 | 2,6 dimethoxyphenol | | -3.1 | -3.6 | - | - |
| 4 | Isoeugenol | | -3.2 | -3.7 | - | - |
| 5 | Vanillin | | -3.4 | - | -2.5 | - |
| 6 | t-Cinnamaldehyde | | - | - | -3.4 | - |
| 7 | Anisole | | - | - | - | -4.5 |
| 8 | Acetophenone | | - | - | - | -6.3 |

Notes: See text for pathway definitions. All k in $s^{-1}$.

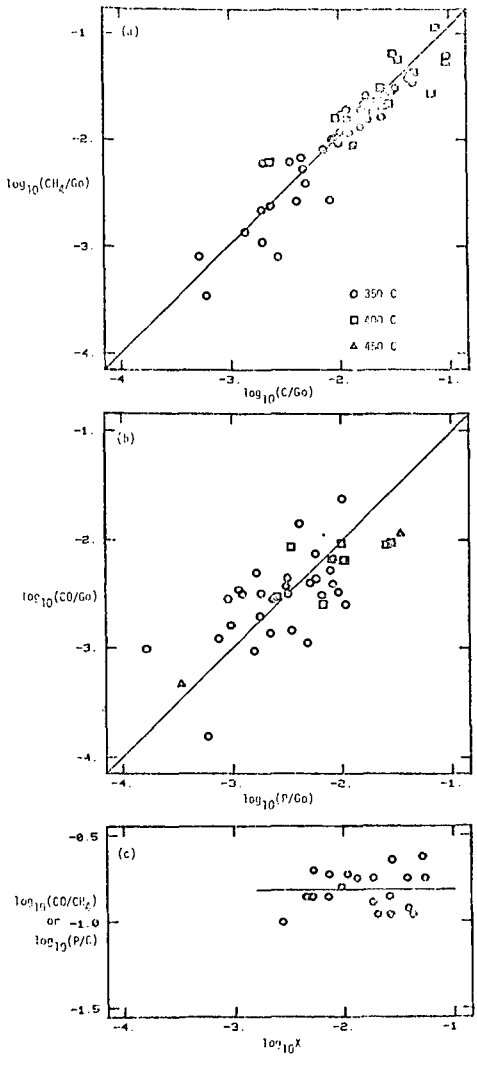


Figure 1. Product relationships in guaiacol pyrolysis:
(a) Methane vs. Catechol
(b) Carbon Monoxide vs. Phenol
(c) (Phenol/Catechol) ratio vs. Substrate conversion

Note: P-Phenol, C-Catechol, Go-Guaiacol,initial, X- Guaiacol conversion

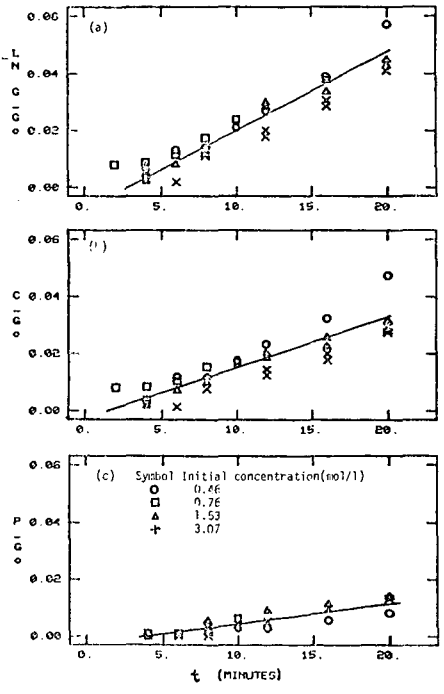


Figure 2. Guaiacol pyrolysis kinetics, T= 350 C:
(a) Substrate disappearance
(b) Catechol appearance
(c) Phenol appearance

| Substrate | Path | $\log_{10}A(s^{-1})$ | $E^*$(kcal/mol) |
|---|---|---|---|
| ○ Guaiacol | R1 | 10.9±0.5 | 43.7±1.4 |
| □ Guaiacol | R2 | 11.5±0.5 | 47.4±1.6 |
| ◇ Anisole | R4 | 12.1±0.8 | 51.4±2.4 |

| Substrate | Path | $\log_{10}A(s^{-1})$ | $E^*$(kcal/mol) |
|---|---|---|---|
| ○ Benzaldehyde | R3 | 9.5±0.8 | 41.5±2.7 |
| □ Acetophenone | R4 | 10.3±1.6 | 50.7±5.8 |

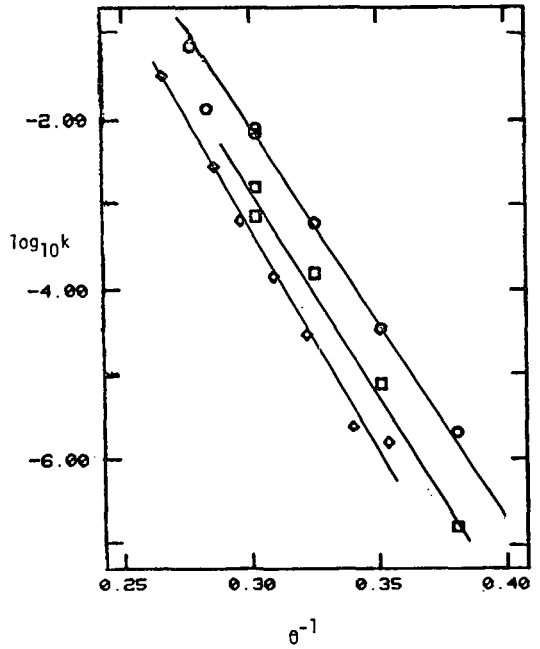


Figure 3. Arrhenius diagram for Guaiacol and Anisole pyrolyses.

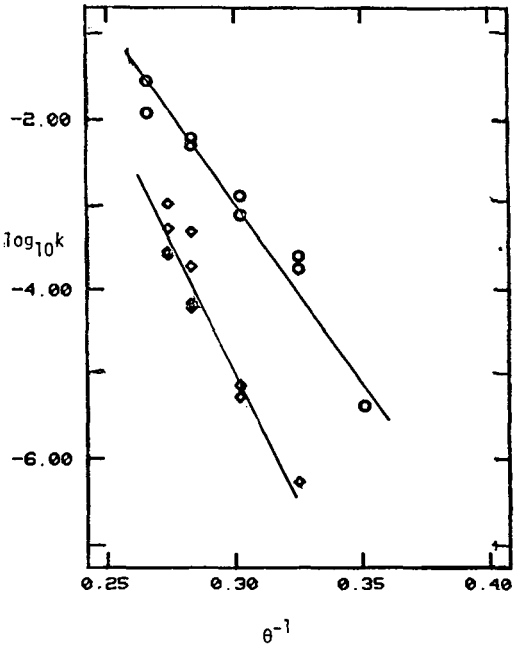


Figure 4. Arrhenius diagram for Benzaldehyde and Acetophenone pyrolyses.